Self-interstitials injection in crystalline Ge induced by GeO_2 nanoclusters

G. G. Scapellato,[1] S. Boninelli,[1] E. Napolitani,[2] E. Bruno,[1] A. J. Smith,[3] S. Mirabella,[1] M. Mastromatteo,[2] D. De Salvador,[2] R. Gwilliam,[3] C. Spinella,[4] A. Carnera,[2] and F. Priolo[1]

[1]*MATIS IMM-CNR and Dipartimento di Fisica e Astronomia, Università di Catania, via S. Sofia 64, 95123 Catania, Italy*

[2]*MATIS IMM-CNR and Dipartimento di Fisica, Università di Padova, via Marzolo 8, 35131 Padova, Italy*

[3]*Ion Beam Centre, The University of Surrey, Guildford, Surrey, GU2 7XH, United Kingdom*

[4]*IMM-CNR, Ottava strada 5, 95121 Catania, Italy*

(Received 1 June 2011; published 5 July 2011)

The effect of O implantation in crystalline Ge on the density of native point defects has been investigated through transmission electron microscopy and B diffusion experiments. Annealing at 650 °C following O implants produces a band of defects (∼5–10 nm), compatible with GeO_2 nanoclusters (NCs). A clear shape transformation from elongated to spherical forms occurs within 2 h, concomitant with a transient enhanced diffusion of B. A large injection of self-interstitials from GeO_2 NCs, giving a vacancy undersaturation, and a long-range migration of self-interstitials are evidenced and discussed.

DOI: 10.1103/PhysRevB.84.024104 PACS number(s): 66.30.J−, 85.40.Ry

I. INTRODUCTION

In the past decade some basic properties of crystalline Ge, among which the formation and migration of point defects (vacancy or self-interstitial), their interactions with impurities, their role in diffusion and activation of dopants, have been the subject of a renewed scientific interest,[1–3] mainly motivated by a low-field carrier mobility larger in Ge than in Si.[4] Such an advantage of Ge over Si together with their structural similarities are opening the route for a wider and gainful use of this semiconductor in the next generation of sub-22 nm complementary metal-oxide-semiconductor (C-MOS) microelectronic devices. However, the knowledge on point defects (PDs) properties and the ability to engineer their distribution is by far less mature in Ge than in Si, limiting any reliable control of dopant activation or diffusion typically mediated by PDs.

Several theoretical works calculated the charge states and the formation and migration energies of vacancies or self-interstitials in Ge for different configurations or Fermi-level positions,[1,5–7] but many experiments are limited to electron irradiation below 100 K.[8–10] At room or higher temperature, vacancies and self-interstitials can be studied in an indirect way, through PDs-assisted migration of impurities. Still, Ge is dominated by vacancies under equilibrium conditions, and self-interstitials do not play a significant role, having a formation energy ∼1 eV larger than vacancies.[1,7] Moreover, Ge itself[11] and most donor impurities diffuse in Ge via a vacancy-donor pair,[12] also responsible for unwanted dopant deactivation.[3,13] Thus, experimental data on vacancy or vacancy-donor pairs can be compared to the calculated ones.[1] The same does not hold for self-interstitials, due to their shortage in Ge crystals.

The modest role of self-interstitials in Ge is also testified by the lack of any self-interstitial-type defects in Ge after Czochralski (Cz) growth[1,4] and by the very small and relatively unstable self-interstitial-type extended defects formed at the end-of-range (EOR) region after amorphization and solid-phase epitaxial regrowth.[14–16] Recently, some progress in understanding the role of self-interstitials in Ge came from investigations on the migration of B, whose diffusivity is the lowest among all the impurities in Ge.[2,17,18] Napolitani *et al.*[16] correlated the evolution of self-interstitial-type EOR defects with the diffusion of very thin B profiles, which supports the self-interstitial mediated diffusion of B in Ge recently proposed in the literature.[3,19] Therefore, B diffusion is a valuable indirect marker for self-interstitials in Ge, as previously studied in Si with a well-established methodology.[20–24]

By using B diffusion, proton irradiation in Ge has been proved to increase the PD density above the equilibrium, leading to a significant radiation enhanced diffusion (RED) of B.[19] The same technique was used to suppress vacancy-mediated diffusion and clustering of P and As.[3,13] Still, under proton irradiation, the enhancement of self-interstitial density lasts for the implantation time, provoking a very weak postimplant transient enhanced diffusion (TED) of B.[19] Typically, damage induced by ion implantation in Ge does not generate visible and stable self-interstitial clusters.[25,26] Even the EOR defects induce a modest self-interstitial enhancement, with a relatively small TED for B, vanishing over 450 °C.[16,27] Thus, PD engineering for a strong self-interstitial supersaturation could create an innovative framework for Ge material, where the diffusion and deactivation of all donor atoms are dominated by vacancies.

In this letter, a significant PDs imbalance in favor of self-interstitials is shown after O implantation in crystalline Ge. Clear evidence of extended defects formed as a consequence of GeO_2 nanoclusters is given, linked to a huge and long-lasting self-interstitial supersaturation at 650 °C verified with B diffusion experiments.

II. EXPERIMENTAL

Cz-Ge ⟨001⟩ crystals (*p* type, resistivity of ∼0.001 Ω/cm) were implanted at room temperature (RT) with 4×10^{14} O/cm^2 ion beam at 235 keV (projected range R_p, ∼450 nm[28]). Some implanted samples were annealed at 650 °C (30–180 min) in ultrapure N_2 flowing gas with a proximity capping with pure Ge samples. Cross-sectional transmission electron microscopy (XTEM) analyses were done with a 200 keV Jeol 2010F instrument, and secondary ion mass spectrometry (SIMS)

were conducted for B and O profiling with a Cameca IMS-4f instrument using a 3 keV O_2^+ or 14.5 keV Cs^+ analyzing beam, respectively.

III. RESULTS AND DISCUSSION

Figure 1 shows the O profile in the Cz-Ge sample before (solid line) and after annealing at 650 °C for 30 (squares) and 120 (triangles) min. The annealing does not induce any O loss, but a significant shrinkage of the O profile (forming a wide peak at around 4/5 of the R_p) is observed, stable up to 3 h at 650 °C. According to the O diffusivity in Ge,[29] after 650 °C for 30 min the diffusion length is ∼700 nm, long enough to justify a complete flattening of the profile (not observed). This behavior recalls what happens in the separation by implanted oxygen (SIMOX) technology used in Si[30] or in high-dose O implantation in Ge,[31] but in our case a clear shift of the O distribution is observed and, moreover, the O implant dose is four orders of magnitude lower. Figures 2(a) and 2(b) show the XTEM of Cz-Ge sample implanted with O and annealed at 650 °C for 30 and 120 min, respectively. In both cases, where O accumulates (around ∼370 nm) many self-interstitial-rich nanoclusters (NCs) are present (5–10 nm in size) whose structure is reported in the high-resolution (HR) images observed along the [011] zone axis [insets (c) and (d)]. After 30 min at 650 °C annealing most NCs show an elongated shape, while after 120 min they have a spherical, crystalline structure. The lattice fringes in correspondence with the NC [inset (d)] strongly differ from those present in the surrounding Ge matrix. In fact, the crystalline structure of the NC, interposed between the Ge crystalline lattice, causes the formation of typical Moiré fringes. As a proof, after indexing the fast Fourier transform [inset (e)] of the HR image of the NC, some supplementary diffraction spots appear, in addition to the Ge crystalline spots. The spot indicated with an arrow in inset (e) is related to the interplanar distance $d = 4.3$ Å, compatible with the {100} lattice planes of the rutile GeO_2.[32] After filtering the HR-TEM with the frequencies characteristic

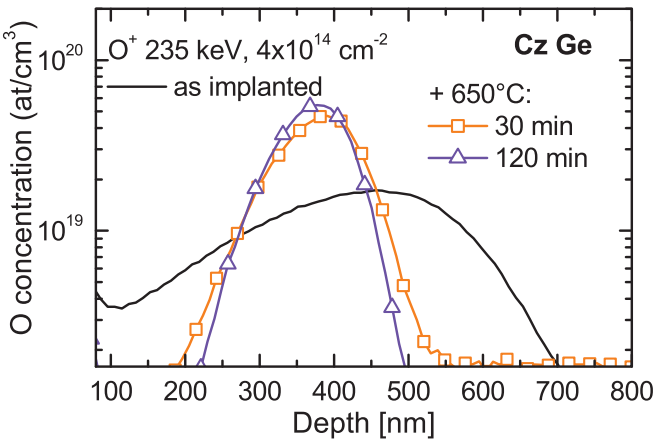

FIG. 1. (Color online) Oxygen profile in the Cz-Ge sample after implantation (O^+ 235 keV, $4 \times 10^{14} cm^{-2}$ at RT, black line) and after annealing at 650 °C for 30 (orange line plus squares) and 120 (violet line plus triangles) min. No oxygen loss occurs during the annealing, while a significant O accumulation is observed at a shallower depth with respect to the implanted profile.

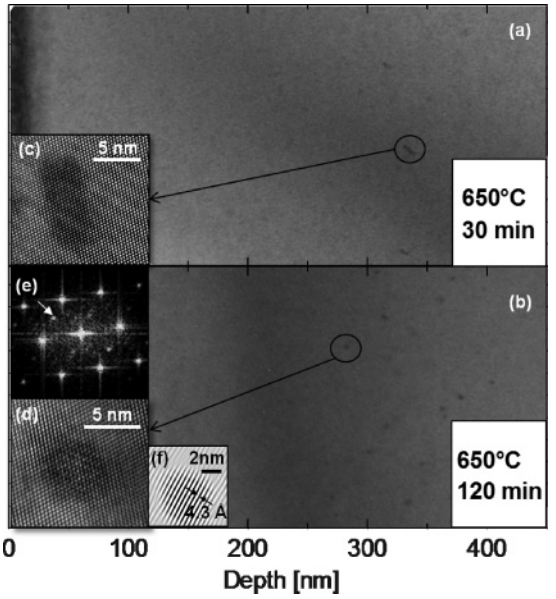

FIG. 2. Cross-sectional TEM micrograph of Cz sample implanted and annealed at 650 °C for (a) 30 min and (b) 120 min, revealing the presence of GeO_2 nanoclusters. (c) and (d) HR-TEM images of typical nanoclusters evidencing the shape transformation between 30 and 120 min. (e) The fast Fourier transform diffraction pattern of the HR image of the cluster (d) with the arrow indicating one of the supplementary diffraction spots of crystalline GeO_2 (see text for details). (f) The image of the cluster showing the planes compatible with {100} GeO_2 planes obtained after filtering the HR-TEM (d).

of these planes, the image of the NC showing the {100} planes has been obtained [inset (f)].

The observed GeO_2 NCs exhibit a thermal stability much larger than the EOR defects in Ge.[16] In order to explain the O accumulation, observed also after 180 min at 650 °C annealing (not shown), it should be noted that: (i) TEM analyses on the as-implanted sample revealed a highly defective crystalline structure, confirming the subamorphizing implant; (ii) the O accumulation region corresponds to the depth along the ion track where the rate of energy loss versus depth (and thus the crystal damage rate) is maximum.[28] Thus, the O accumulation can be promoted by some crystal defects (distorted or broken bonds, PDs) created by the implantation and acting as stable gettering centers for O, as the O-V center.[33] Recently, it was argued that at temperatures as low as 150 K self-interstitials can interact with interstitial O (O_i) forming self-interstitial-O_i complexes, leading to self-interstitial-$(O_i)_2$ complexes above 50 °C.[34] Upon annealing at 650 °C, such self-interstitial-$(O_i)_2$ complexes could grow into elongated or more stable spherical NCs of GeO_2. Such a change in shape agrees well with the hypothesis assumed to simulate infrared spectra of oxide precipitates in Cz-Ge in Ref. 35, according to which the shape of GeO_2 clusters should be spherical and disclike at 560 °C but only spherical at 620 °C.

To verify if the formation of GeO_2 NCs affects the PD equilibrium density, we have employed B diffusion. The same experimental procedure of O implantation and annealing has been performed on a molecular beam epitaxy grown Ge (MBE-Ge) containing a B multidelta structure (five narrow B-doped layers B-δ, positioned 200 nm apart) with growth and

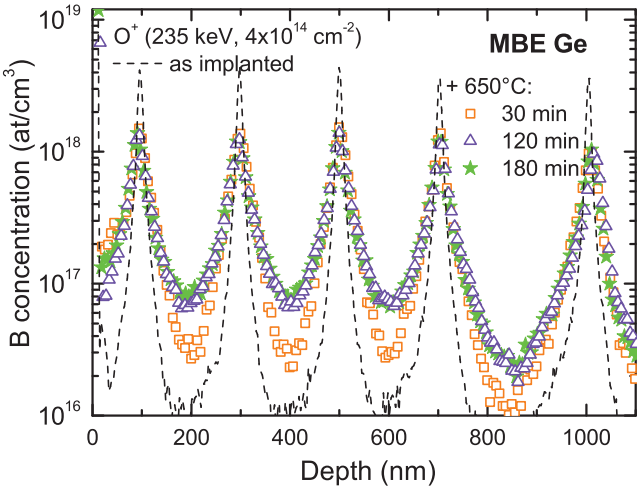

FIG. 3. (Color online) Boron profiles in MBE-Ge sample after implantation (black dashed line), and after annealing at 650 °C for 30 (orange open squares), 120 (violet open triangles), and 180 (green stars) min. A homogeneous broadening of the B profiles is observed, evidencing a transient enhanced diffusion of B lasting less than 120 min at 650 °C.

pre-annealing details as in Ref. 19. SIMS analyses were used to measure B diffusion, whose simulation based on the model of Cowern *et al.*[20,24,36] allows evidence of changes of self-interstitial density in Ge.[3,16,19,37]

Figure 3 shows the B profiles of the MBE-Ge after implantation (dashed line) and after annealing at 650 °C for 30 (squares), 120 (triangles), and 180 (stars) min. A clear broadening of B-δs is visible already after 30 min at 650 °C (for which the equilibrium diffusion is negligible[38]), going on up to 120 min. The as-implanted profile is not significantly larger than the as-grown one (not shown). Thus, B undergoes an evident transient enhanced diffusion related to the O implantation and exhausted after 120 min at 650 °C. In addition, such TED of B is homogeneous from the surface down to 1.2 μm, not limited to the region of GeO_2 NCs. A Ne implantation, whose energy and fluence (265 keV, $3 \times 10^{14}/cm^2$) were chosen to give a similar crystal damage of the O implant (since the nuclear energy loss of O and Ne implantations is similar[28]), was performed and followed by 650 °C annealing. In this sample a negligible broadening of B profiles is observed [circles in Fig. 4(a)]. This counterproofs that the injection of interstitials is related to the presence of O. A strong relation between the formation of the GeO_2 NCs and a significant self-interstitial supersaturation is observed, affecting a Ge region larger than 1 μm.

In Si, a self-interstitial supersaturation is typically produced during surface oxidation because of the different densities of Si and SiO_2.[39] The consequent stress at the Si/SiO_2 interface is partially released by injecting self-interstitials, responsible for the oxidation enhanced diffusion (OED) of B.[39] The same approach in Ge is not effective because of GeO desorption.[40,41] Still, in our case the embedded GeO_2 NCs could act as the self-interstitial source. Based on the different Ge densities in Ge and in GeO_2 (4.8 or 2.4×10^{22} Ge/cm^3), the volume per Ge atom in the oxide is twice than in bulk, and the stress at the NC surface can be released by injecting self-interstitials in the surrounding lattice. The homogeneous broadening of a B multidelta indicates that self-interstitials are reflected by the surface, causing a flat self-interstitial supersaturation, in agreement with Refs. 3 and 13. Assuming that self-interstitials are created at ~370 nm, given the B diffusion at ~1000 nm (deepest B-δ in Fig. 3) just after 30 min, one can evaluate $\sim 2 \times 10^{-12}$ cm^2/s as a lower estimate for self-interstitial diffusivity (D_I) at 650 °C, (using $\lambda = \sqrt{D_I t}$). These data show that, once formed, self-interstitials can affect the Ge lattice at long distances and in a non-negligible way, remarking that the weak role of self-interstitials in Ge can be related to their quite large formation energy with respect to vacancies.

In order to quantitatively study the self-interstitial supersaturation, we fitted the B profiles by means of a χ^2 optimization of numerical simulations based on the g-λ diffusion model,[20,24,36] successfully applied also for B diffusion in Ge.[16,19] Here, g gives the B-self-interstitial interaction rate leading to one B diffusion event, while λ is the mean length of

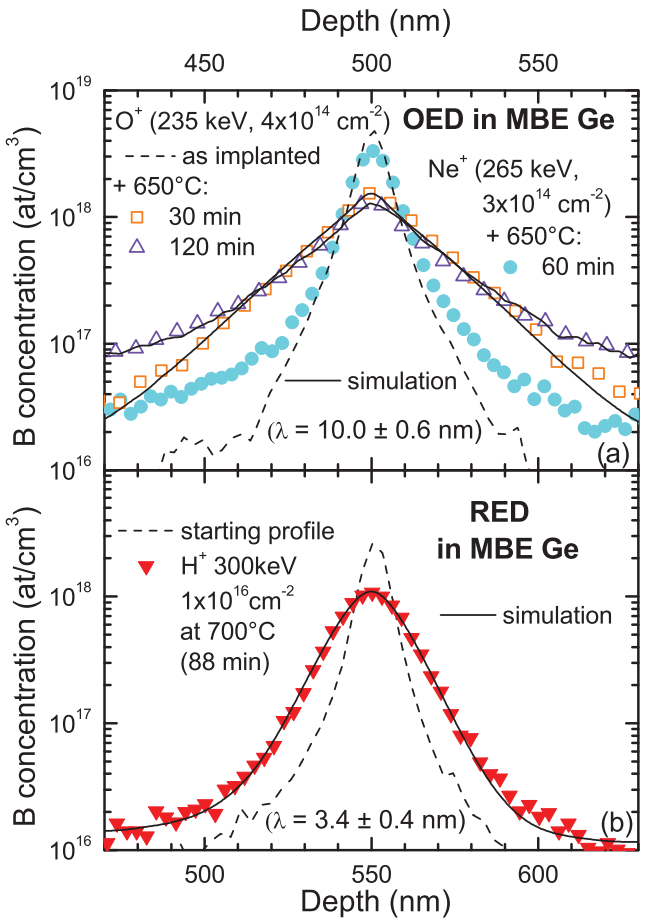

FIG. 4. (Color online) (a) Oxidation-enhanced diffusion produces non-Gaussian shape: B profiles in the MBE-Ge sample after O implantation (black dashed line) and after annealing at 650 °C for 30 (orange open squares) and 120 (violet open triangles) min compared with B profile after Ne implantation and annealing at 650 °C for 60 min (cyan closed circles). (b) Radiation-enhanced diffusion produces Gaussian shape: B profiles before (black dashed line) and after (red closed triangles) proton irradiation at 700 °C (H^+ 300 keV, 1×10^{16} cm^{-2}). Solid lines are simulations based on g-λ diffusion model.

B migration per each diffusion hop. B diffusivity is given by $D_B = g\lambda^2$. The model was applied to all the B δs, and Fig. 4(a) shows the simulation curves (continuous lines) for 30 and 120 min annealing, accounting for the very good quality of the fits. The average number of diffusion events (gt, t is the annealing time) for each B atom in the 0–30 and 30–120 min annealing are 2.39 ± 0.17 and 0.24 ± 0.04, respectively, confirming the TED of B. Given the model results, and extrapolating at 650 °C D_B in equilibrium conditions reported in Ref. 42, the average enhancement of D_B in the 0–30 min annealing is $\sim 2 \times 10^5$. Actually, the OED of B in Si is much lower [D_B enhancement of ~10 (Refs. 43 and 44)], but the equilibrium self-interstitial density in Si is much larger than in Ge, weakening the effect of self-interstitial injection during OED in Si. In our case, if all the implanted O atoms are involved in GeO_2 clusters (5 nm in diameter and distributed over the 150-nm-wide peak of Fig. 1), a cluster density of $\sim 1 \times 10^{16}$ cm^{-3} is expected. This is only a lower limit, since smaller GeO_2 clusters cannot be excluded. Thanks to the high surface-to-volume ratio, the self-interstitial injection by the GeO_2 NCs can be very effective, justifying the larger self-interstitial enhancement in our case.

Diffused profile of Fig. 4(a) shows a non-Gaussian shape, with large exponential tails revealing a quite long migration length ($\lambda \sim 10$ nm). Under equilibrium condition, at 755 °C we measured a ~10 times lower λ (Ref. 19). RED of B has been found under proton irradiation at 700 °C [Fig. 4(b)] with $\lambda \sim 3$ nm, leading to the Gaussian shape of the diffused profile. Despite the similar temperatures, a significant disparity in λ is observed, indicating that the migration length per each B diffusion event is markedly longer in the presence of GeO_2 NCs compared to the equilibrium or RED cases. Such dissimilarity is also evident from the diverse shapes of the two diffused profiles [Figs. 4(a)–4(b)]. It should be noted that λ could be related to the availability of vacancies, which can trap the diffusing B atom, reducing the migration length. So the longer λ in the presence of GeO_2 NCs is compatible with an undersaturation of vacancies, probably due to recombination with self-interstitials injected from GeO_2 NCs.

IV. CONCLUSIONS

In conclusion, we showed that O implantation in crystalline Ge followed by a 650 °C annealing induces the formation of GeO_2 nanoclusters. These defects, between 30 and 120 min at 650 °C, undergo a structural transformation from an elongated shape to a spherical form, compatible with that of crystalline GeO_2. At the same time, a large enhancement of self-interstitial density, exhausted after 120 min at 650 °C, is revealed by B diffusion experiments. It is proposed that a significant self-interstitial injection occurs because of the formation of the GeO_2 NCs, similar to what happens in Si under surface oxidation. Based on the B diffusion shape and its simulations, this system is compatible with a significant vacancy impoverishment. Such a noteworthy imbalance of PD density in favor of self-interstitials allows a significant change in the basic properties of crystalline Ge, dominated by vacancies under equilibrium conditions.

ACKNOWLEDGMENTS

The authors wish to thank C. Percolla, S. Tatì (CNR-IMM MATIS), and R. Storti (University of Padova) for technical contribution. S.B. is grateful to C. Bongiorno (CNR-IMM) for scientific discussions. This work has been supported in part by the European Community as an integrating activity support of public and industrial research using ion beam technology (SPIRIT) under EC Contract No. 227012.

[1] J. Vanhellemont, P. Spiewak, and K. Sueoka, J. Appl. Phys. **101**, 036103 (2007), and references therein.
[2] C. Janke, R. Jones, S. Oberg, and P. R. Briddon, Phys. Rev. B **77**, 075208 (2008).
[3] H. Bracht, S. Schneider, J. N. Klug, C. Y. Liao, J. Lundsgaard Hansen, E. E. Haller, A. Nylandsted Larsen, D. Bougeard, M. Posselt, and C. Wündisch, Phys. Rev. Lett. **103**, 255501 (2009), and references therein.
[4] C. Claeys and E. Simoen, *Germanium-Based Technologies: From Materials to Devices* (Elsevier, Amsterdam, 2007), and references therein.
[5] A. J. R. da Silva, A. Janotti, A. Fazzio, R. J. Baierle, and R. Mota, Phys. Rev. B **62**, 9903 (2000).
[6] M. Dionizio Moreira, R. H. Miwa, and P. Venezuela, Phys. Rev. B **70**, 115215 (2004).
[7] A. Carvalho, R. Jones, C. Janke, J. P. Goss, P. R. Briddon, J. Coutinho, and S. Öberg, Phys Rev. Lett. **99**, 175502 (2007).
[8] H. Haesslein, R. Sielemann, and C. Zistl, Phys. Rev. Lett. **80**, 2626 (1998).
[9] P. Ehrhart and H. Zillgen, J. Appl. Phys. **85**, 3503 (1999).
[10] J. Fage-Pedersen, A. Nylandsted Larsen, and A. Mesli, Phys. Rev. B **62**, 10116 (2000).
[11] E. Hüger, U. Tietze, D. Lott, H. Bracht, D. Bougeard, E. E. Haller, and H. Schmidt, Appl. Phys. Lett. **93**, 162104 (2008).
[12] S. Brotzmann, H. Bracht, J. Lundsgaard Hansen, A. Nylandsted Larsen, E. Simoen, E. E. Haller, J. S. Christensen, and P. Werner, Phys. Rev. B **77**, 235207 (2008).
[13] S. Schneider and H. Bracht, Appl. Phys. Lett. **98**, 014101 (2011).
[14] D. P. Hickey, Z. L. Bryan, K. S. Jones, R. G. Elliman, and E. E. Haller, Appl. Phys. Lett. **90**, 132114 (2007).
[15] S. Koffel, N. Cherkashin, F. Houdellier, M. J. Hytch, G. Benassayag, P. Scheiblin, and A. Claverie, J. Appl. Phys. **105**, 126110 (2009).
[16] E. Napolitani, G. Bisognin, E. Bruno, M. Mastromatteo, G. G. Scapellato, S. Boninelli, D. De Salvador, S. Mirabella, C. Spinella, A. Carnera, and F. Priolo, Appl. Phys. Lett. **96**, 201906 (2010).
[17] H. Bracht and S. Brotzmann, Mater. Sci. Semicond. Process. **9**, 471 (2006), and references therein.
[18] A. Chroneos, P. B. Uberuaga, and R. W. Grimes, J. Appl. Phys. **102**, 083707 (2007).

[19]E. Bruno, S. Mirabella, G. G. Scapellato, G. Impellizzeri, A. Terrasi, F. Priolo, E. Napolitani, D. De Salvador, M. Mastromatteo, and A. Carnera, Phys. Rev. B **80**, 033204 (2009).
[20]N. E. B. Cowern, K. T. F. Janssen, G. F. A. van de Walle, and D. J. Gravesteijn, Phys. Rev. Lett. **65**, 2434 (1990).
[21]P. A. Stolk, H. J. Gossmann, D. J. Eaglesham, D. C. Jacobson, C. S. Rafferty, G. H. Gilmer, M. Jaraız, J. M. Poate, H. S. Luftman, and T. E. Haynes, J. Appl. Phys. **81**, 6031 (1997).
[22]S. Mirabella, A. Coati, D. De Salvador, E. Napolitani, A. Mattoni, G. Bisognin, M. Berti, A. Carnera, A. V. Drigo, S. Scalese, S. Pulvirenti, A. Terrasi, and F. Priolo, Phys. Rev. B **65**, 45209 (2002).
[23]E. Napolitani, D. De Salvador, R. Storti, A. Carnera, S. Mirabella, and F. Priolo, Phys. Rev. Lett. **93**, 055901 (2004).
[24]D. De Salvador, E. Napolitani, S. Mirabella, G. Bisognin, G. Impellizzeri, A. Carnera, and F. Priolo, Phys. Rev. Lett. **97**, 255902 (2006).
[25]G. Bisognin, S. Vangelista, M. Berti, G. Impellizzeri, and M. G. Grimaldi, Thin Solid Films **518**, 2326 (2010).
[26]S. Koffel, P. Scheiblin, A. Claverie, and G. Benassayag, J. Appl. Phys. **105**, 013528 (2009).
[27]F. Panciera, P. F. Fazzini, M. Collet, J. Boucher, E. Bedel, and F. Cristiano, Appl. Phys. Lett. **97**, 012105 (2010).
[28]J. F. Ziegler, J. P. Biresack, and U. Littmark, *The Stopping and the Range of Ions in Solids* (Pergamon, New York, 1985).
[29]V. Gusakov, J. Phys. Cond. Matt. **17**, S2285 (2005).
[30]Y. Li, J. A. Kilner, P. L. F. Hemment, A. K. Robinson, J. P. Zhang, K. J. Reeson, C. D. Marsh, and G. R. Booker, Nucl. Instr. and Meth. Phys. Res. B **64**, 750 (1992).
[31]N. M. Ravindra, T. Fink, W. Savin, T. P. Sjoreen, R. L. Pfeffer, L. G. Yerke, R. T. Lareau, J. G. Gualtieri, R. Lux, and C. Wrenn, Nucl. Instr. and Meth. Phys. Res. B **46**, 409 (1990).
[32]T. I. Milenov, V. I. Dimov, P. M. Rafailov, and M. M. Gospodinov, Appl. Phys. A **92**, 643 (2008).
[33]A. Chroneos, C. A. Londos, and H. Bracht, Mater. Sci. Eng. B **176**, 453 (2011).
[34]V. P. Markevich, A. R. Peaker, S. B. Lastovskii, L. I. Murin, V. V. Litvinov, V. V. Emtsev, and L. Dobaczewski, Phys. B **404**, 4533 (2009).
[35]O. De Gryse, P. Vanmeerbeek, J. Vanhellemont, and P. Clauws, Phys. B **376–377**, 113 (2006).
[36]N. E. B. Cowern, G. F. A. van de Walle, D. J. Gravesteijn, C. J. Vriezema, Phys. Rev. Lett. **67**, 212 (1991).
[37]E. Bruno, S. Mirabella, G. G. Scapellato, G. Impellizzeri, A. Terrasi, F. Priolo, E. Napolitani, D. De Salvador, M. Mastromatteo, and A. Carnera, Thin Solid Films **518**, 2386 (2010).
[38]S. Uppal, A. F. W. Willoughby, J. M. Bonar, N. E. B. Cowern, T. Grasby, R. J. H. Morris, and M. G. Dowsett, J. Appl. Phys. **96**, 1376 (2004).
[39]H. Kageshima, M. Uematsu, and K. Shiraishi, Microelectron. Eng. **59**, 301 (2001).
[40]A. Molle, Md. N. K. Bhuiyan, G. Tallarida, and M. Fanciulli, Appl. Phys. Lett. **89**, 083504 (2006).
[41]S. K. Wang, K. Kita, C. H. Lee, T. Tabata, T. Nishimura, K. Nagashio, and A. Toriumi, J. Appl. Phys. **108**, 054104 (2010).
[42]S. Uppal, A. F. W. Willoughby, J. M. Bonar, A. G. R. Evans, N. E. B. Cowern, R. Morris, and M. G. Dowsett, J. Appl. Phys. **90**, 4293 (2001).
[43]N. Cowern and C. Rafferty, Mater. Res. Soc. Bull. **25**, 39 (2000).
[44]M. Miyake, J. Appl. Phys. **57**, 1861 (1985).